iScience

CellPress
OPEN ACCESS

Article

Elevated high-mannose N-glycans hamper endometrial decidualization

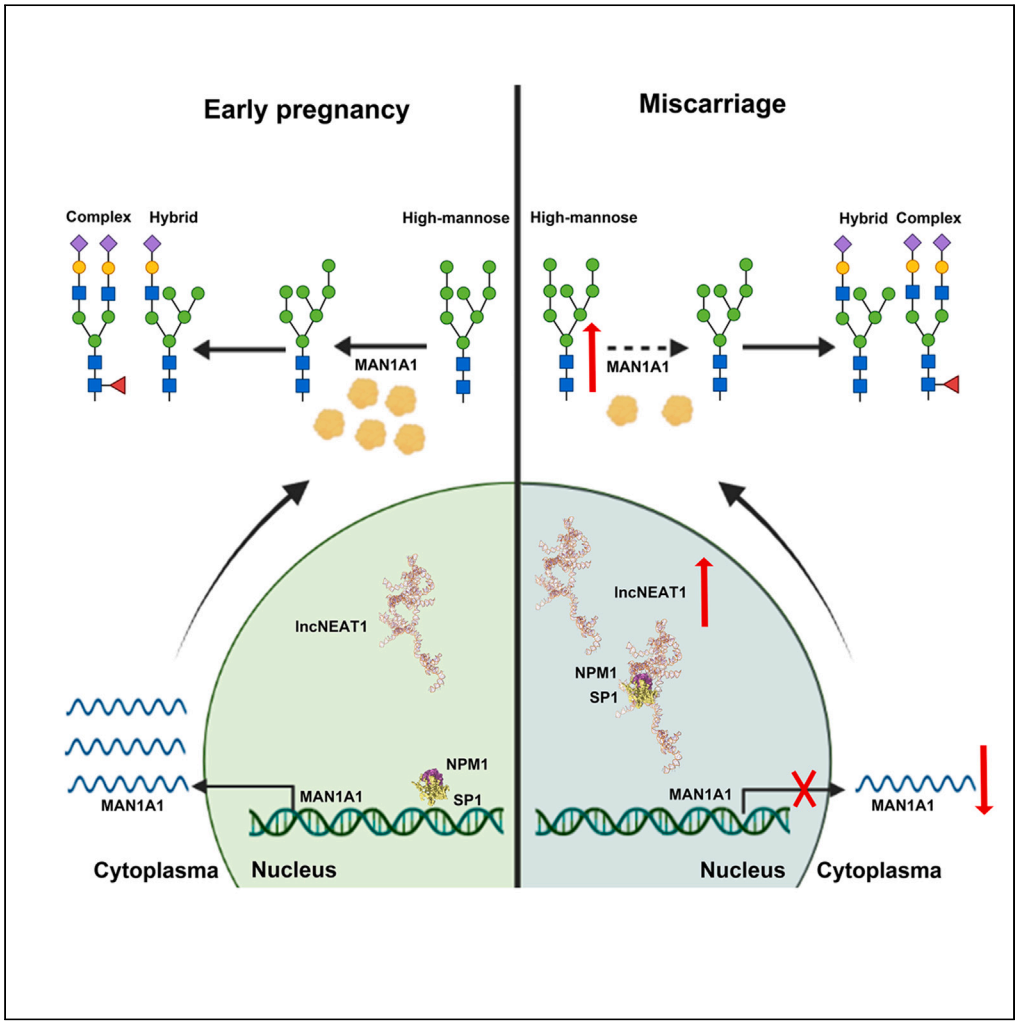

Siyi Chen, Aihui Zhang, Na Li, Hongpan Wu, Yaqi Li, Shuai Liu, Qiu Yan

liushuai@dmu.edu.cn (S.L.)
yanqiu@dmu.edu.cn (Q.Y.)

Highlights

Elevated high-mannose N-glycans and decreased MAN1A1 in miscarriage patients' decidua

Silencing MAN1A1 increases high-mannose N-glycan and inhibits endometrial decidualization

Increased lncNEAT1 level in the decidual tissues of miscarriage patients

lncNEAT1 and NPM1-SP1 interaction decreases MAN1A1 expression and hampers decidualization

Chen et al., iScience *26*, 108170
November 17, 2023
https://doi.org/10.1016/j.isci.2023.108170

iScience

CellPress
OPEN ACCESS

Article

Elevated high-mannose N-glycans hamper endometrial decidualization

Siyi Chen,[1] Aihui Zhang,[1] Na Li,[1] Hongpan Wu,[1] Yaqi Li,[1] Shuai Liu,[1,*] and Qiu Yan[1,2,*]

SUMMARY

Decidualization of endometrial stromal cells is a hallmark of endometrial receptivity for embryo implantation, and dysfunctional decidualization is associated with pregnancy failure. Protein glycosylation is an important posttranslational modification that affects the structure and function of glycoproteins. Our results showed that high-mannose epitopes were elevated in the decidual tissues of miscarriage patients compared with early pregnant women by Lectin microarray. Furthermore, the level of mannosyl-oligosaccharide α-1,2 mannosidase IA (MAN1A1), a key enzyme for high-mannose glycan biosynthesis, was decreased in the decidual tissues of miscarriage patients. Screening of lncRNAs showed that lncNEAT1 level was increased in the serum and decidua of miscarriage patients, and negatively correlated with MAN1A1 expression. The results also revealed that specific binding of lncNEAT1 with nucleophosmin (NPM1)-SP1 transcription complex inhibited MAN1A1 expression and hampered endometrial decidualization and embryo implantation potential. The study suggests the new insights into the function of high-mannose glycans/MAN1A1 modification during endometrial decidualization.

INTRODUCTION

Spontaneous pregnancy loss is a common pregnancy disorder and affects approximately 15% of the general population worldwide.[1] Endometrial dysfunction and poor embryo quality are considered as the crucial causes of pregnancy loss. Recently, increasing lines of evidence have indicated that deficient decidualization of the endometrium leads to implantation failure or embryo developmental delay, resulting in miscarriage and infertility.[2,3] Decidualization of endometrial stromal cells is the hallmark of tissue remodeling, which guarantees proper feto-maternal interface formation, supports embryo implantation, and accommodates placental development. During decidualization, endometrial stromal cells undergo cellular morphology and function changes. From morphological side, cells gradually become round from a long spindle shape, and nuclei are enlarged with binuclear or multinuclear occurrence. From functional side, decidual stromal cells produce decidua-specific glycoproteins in physiological pregnancy and decidualization *in vitro* by medroxyprogesterone 17-acetate (MPA) and dibutyryl cAMP (dbcAMP).[4] For example, calreticulin upregulates decidualization by folding and quality control of the glycoproteins.[5] Glycosylated osteopontin is highly expressed in the decidual stromal cells, and promotes the expression of decidualization- and angiogenesis-related genes.[6] Prolactin (PRL) and insulin-like growth factor-binding protein 1 (IGFBP-1) are the essential decidual markers to evaluate the decidual response of human endometrial stromal cells.[7] Studies have shown that the malfunction of many implantation molecules, including cytokines, transcription factors, and hormones, are associated with abnormal decidualization.[8–10] However, the linked glycobiological pathogenesis and mechanism in decidualization defects are largely unknown.

Glycosylation is an important posttranslational modification. It is mainly divided into N-linked and O-linked glycosylation. N-glycosylation occurs when the sugar chain is covalently linked to the peptide at Asn-X-Ser/Thr glycosylation site. It contains three types: high-mannose, complex, and hybrid N-glycans. High-mannose biosynthesis starts from the outer endoplasmic reticulum (ER), and is finally modified in the Golgi apparatus (Golgi). Glycotransferases and glycosidases are mainly responsible for glycan biosynthesis. The synthesis of high-mannose N-glycans is a multistep process, and requires mannosyltransferases (ALGs, ALG1, 2, 3, 9, 11, 12) and mannosidases (MANs, MAN1B1, MAN1A1, 2, MAN1C1, and MAN2A1, 2), as well as glucosyltransferases (ALG6, 8, 10). They catalyze the addition and deletion of UDP-mannose and glucose, respectively.[11–13] Among them, MAN1A1 is a mannosidase that cleaves α1,2-glycosidic bonds from high-mannose glycans, which further contributes to the modification and synthesis of complex or hybrid N-glycans. MAN1A1 plays an important role in the physiological processes. It is reported that MAN1A1 is involved in the adhesion function of endothelial cells by regulating surface high-mannose glycans.[14] However, the role and regulatory mechanism of MAN1A1 on high-mannose N-glycans in reproduction remains unclear.

Long noncoding RNAs (lncRNAs) are a class of RNAs with a length of more than 200 nucleotides. LncRNAs regulate gene expression by chromatin remodeling, transcriptional activation/interference, and mRNA processing and translation by interaction with DNA, mRNA,

[1]Liaoning Provincial Core Lab of Glycobiology and Glycoengineering, College of Basic Medical Science, Department of Biochemistry and Molecular Biology, Dalian Medical University, Dalian 116044, China
[2]Lead contact
*Correspondence: liushuai@dmu.edu.cn (S.L.), yanqiu@dmu.edu.cn (Q.Y.)
https://doi.org/10.1016/j.isci.2023.108170

microRNA, and protein.[15,16] LncRNAs are related to many biological functions, such as cell proliferation, migration, apoptosis, X chromosome inactivation, gene imprinting, and stem cell transformation.[17–19] Increasing evidence also proposes the crucial role of lncRNAs in reproductive processes. For example, lncDANCR, lncMEG8, and lncTCL6 are involved in proliferation, invasion, and migration of trophoblasts.[20–22] lncH19 and lncTNUAR play important roles in endometrial receptivity.[23,24] In addition, lncRNAs regulate multiple steps of the biosynthesis of N- and O-glycans. The correlation between lncRNAs and glycosylation has been reported; lncPSMA3-AS1 promotes cell proliferation, migration, and invasion in ovarian cancer by sponging miR-378a-3p which targets N-acetylgalactosaminyltransferase 3.[25] Para-nuclear assembled transcript 1 (lncNEAT1) is mainly expressed in the nucleus and affects transcription process. It has been reported that downregulated lncNEAT1 promotes proliferation, migration, and invasion of trophoblast cells, and alleviates development of preeclampsia.[26] However, the expression pattern and regulatory target of lncNEAT1 in endometrial decidualization have not been reported.

In this study, we aimed to uncover the function and underlying molecular mechanism of mannosylation in human endometrial stromal decidualization. Employing Lectin microarray, we found increased high-mannose glycans and concomitant reduction of MAN1A1 in the decidual tissues of miscarriage patients compared with early pregnant women. The abnormally elevated high mannosylation by MAN1A1 downregulation inhibited decidualization. Screening of lncRNAs revealed that lncNEAT1 was increased in the decidual tissues of miscarriage patients. Furthermore, the results showed that lncNEAT1 interacted with NPM1-SP1 transcription complex and inhibited MAN1A1 expression, thereby hampering endometrial decidualization and embryo implantation.

RESULTS

Increased high-mannose glycans and decreased MAN1A1 in the decidual tissues of miscarriage patients

To reveal the glycosylation traits of human decidualization, Lectin microarray was employed to acquire the glycomic profile and compare the differential glycan epitopes in the decidual tissues of healthy early pregnant women and miscarriage patients (Figure S1). Based on the high affinity of lectins for recognizing and binding with the specific glycan structure, the mannose level was generally increased in the decidua of miscarriage patients compared with that in early pregnant women. Among them, the mannose-rich glycans recognized by NPA, HHL, LCHA, CALSEPA, Galanthus nivalis lectin (GNA), PSA, and BC2LA were significantly increased in the decidua of the miscarriage group as shown in bar graph, and other lectins showed no statistical changes. Lectin detection signal of GRFT and ConA showed high variability or inconsistencies, and further confirmation was needed (Figure 1A). GNA recognizing specifically high-mannose N-glycans presented the highest level, and showed the most obvious change between healthy and miscarriage endometrium, thus selected as the candidate for further study. Lectin blot also confirmed that the level of high-mannose was significantly increased in the decidual tissues of miscarriage (Figure 1B). Immunohistochemical staining indicated that high-mannose was mainly located in the endometrial stromal cells, and the level was lower in secretory phase compared with proliferative phase of non-pregnant women (Figure S2A). Furthermore, the level of high-mannose in endometrium of miscarriage group was significantly higher than that in early pregnant group (Figure 1C).

The synthesis of high-mannose N-glycans is a multistep process, and requires the participation of many specific enzymes (Figure 1D). To explore the regulatory mechanism of elevated high-mannose in the decidual tissues of miscarriage patients, we compared the levels of eight ALGs and six MANs including ER α1,2-mannosidase I (ERManI: MAN1B1) and Golgi α-mannosidases I (GolgiManI: MAN1A1, MAN1C1, MAN1A2) and Golgi α-mannosidases II (GolgiManII: MAN2A1, MAN2A2)[27] in the decidual tissues of early pregnant women and miscarriage patients by qPCR. The results showed that the mRNA levels of MAN1A1, MAN1C1, MAN2A1, and MAN2A2 were decreased, and MAN1B1 and MAN1A2 were increased. The data suggested multiple mannosidases were likely to be involved in the decidualization regulation (Figure 1E). Western blot results confirmed the reduction of MAN1A1 in miscarriage decidua compared with healthy control (Figure 1F). Immunohistochemical staining showed that MAN1A1 was mainly located in the stromal cells of endometrium, and its expression was higher in secretory phase compared with proliferative phase of non-pregnant women (Figure S2B). Because the alteration of MAN1A1 in the decidualization of endometrial stromal cells, it was identified as a target in this study. The expression of MAN1A1 was decreased in the decidua of miscarriage compared with early pregnancy (Figure 1G). It was also found that the increased ALG12 and MAN1A2 were mainly located in the glandular epithelium of endometrium, indicating that they maybe participated in regulation of the epithelial function (Figures S3A and S3B). MAN1C1 was distributed both in the glandular epithelium and stroma (Figure S3C). MAN2A1 and MAN2A2 act on α1,3-/α1,6-linked mannose in the synthesis of hybrid glycans, and the decreased expression in the decidual tissues of miscarriage patients may contribute to accumulative high-mannose glycans. The results suggested that the increase in high-mannose glycans and decrease in MAN1A1 expression were associated with pregnancy failure.

Silencing MAN1A1 increases high-mannose synthesis and inhibits decidualization of endometrial stromal cells

Having disclosed the differential high-mannose N-glycans and MAN1A1 alteration traits in decidua, we further explored the function of high mannosylation/MAN1A1 during decidualization *in vitro*. Firstly, MAN1A1-siRNA and MAN1A1-cDNA transfection decreased and increased MAN1A1 expression in mRNA and protein levels of human endometrial stromal cells (HESCs), respectively (Figures 2A–2D). Meanwhile, the biosynthesis of high-mannose was correspondingly enhanced or inhibited after MAN1A1-siRNA or MAN1A1-cDNA transfection (Figure S4). Then, we investigated the roles of MAN1A1 and high-mannose in decidualization. HESCs were artificially decidualized by treatment with MPA and dbcAMP *in vitro*. The results showed that MAN1A1 and the main decidual markers PRL and IGFBP-1 were significantly increased in mRNA and protein levels (Figures S5A and S5B), and cell morphology showed typical alterations (a long shuttle to oblate shape, and cell volume enlargement) (Figure S5C), which indicated that decidua induction in HESCs was successful. Moreover, MAN1A1-siRNA inhibited the expression of MAN1A1, PRL, and IGFBP-1, while MAN1A1-cDNA rescued the inhibitory effect (Figures 2F and 2G). Meanwhile, the high-mannose

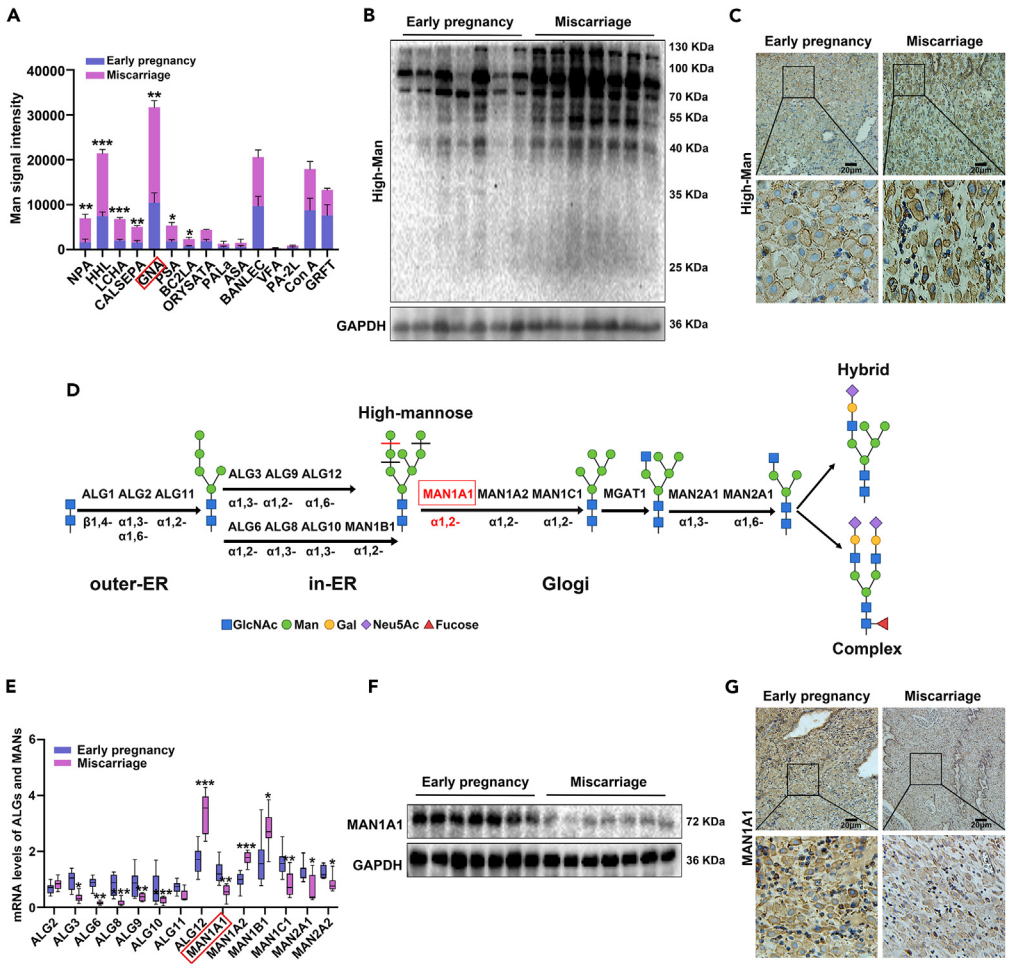

Figure 1. Increased high-mannose glycans and decreased MAN1A1 in the decidual tissues of miscarriage patients

(A) Analysis of differential mannose-specific lectins in the bar graph. GNA: Galanthus nivalis lectin.

(B and C) Lectin blot and immunohistochemical staining analysis of high-mannose glycans in the decidual tissues of early pregnant women (n = 7) and miscarriage patients (n = 7).

(D) Schematic diagram of mannosyltransferases (ALGs) and mannosidases (MANs) catalyzing N-glycosylation synthesis by BioRender.

(E) qPCR analysis of ALGs and MANs in the decidual tissues of early pregnancy and miscarriage.

(F and G) Western blot and immunohistochemical staining analysis of MAN1A1 in the decidual tissues of early pregnant women and miscarriage patients. Scale bars, 20 μm *p < 0.05, **p < 0.01, ***p < 0.001.

biosynthesis showed the opposite change with MAN1A1 and decidual markers (Figure 2E). Immunofluorescent staining showed that MAN1A1 was mainly located in Golgi apparatus. In addition, MAN1A1-siRNA significantly decreased decidualization, and MAN1A1-cDNA rescued the inhibitory effect (Figures 2H–2J). Here, we also checked the complex N-glycans by Lectin blot with PHA-E+L, and found that downregulated MAN1A1 hampered complex N-glycans biosynthesis (Figure S6), which indicated that the N-glycosylation pathway was blocked at high-mannose stage, and facilitated decidualization.

Increased lncNEAT1 level in the decidual tissues of miscarriage patients

LncRNAs play important roles by regulating target gene expression in reproduction. In the current study, we hypothesized that specific lncRNA was involved in decidualization by regulating the expression of MAN1A1. Serum samples were collected from healthy and infertile women for RNA sequencing, and 10,975 upregulated and 6,419 downregulated lncRNAs were obtained. Correlation analysis was made in accordance with MEM database (https://biit.cs.ut.ee/mem/) and R language (robust rank aggregation). A total of 293 lncRNAs were correlated with MAN1A1 (p < 0.001). Combined with lncRNA array results, 101 lncRNAs were correlated with MAN1A1 by correlation analysis, which was shown in Venn diagram (Figure 3A). Among them, 19 significantly downregulated lncRNAs and 22 significantly upregulated lncRNAs (fold change > 2) were identified in volcano plot (Figure 3B). In addition, 22 significantly upregulated lncRNAs were functionally

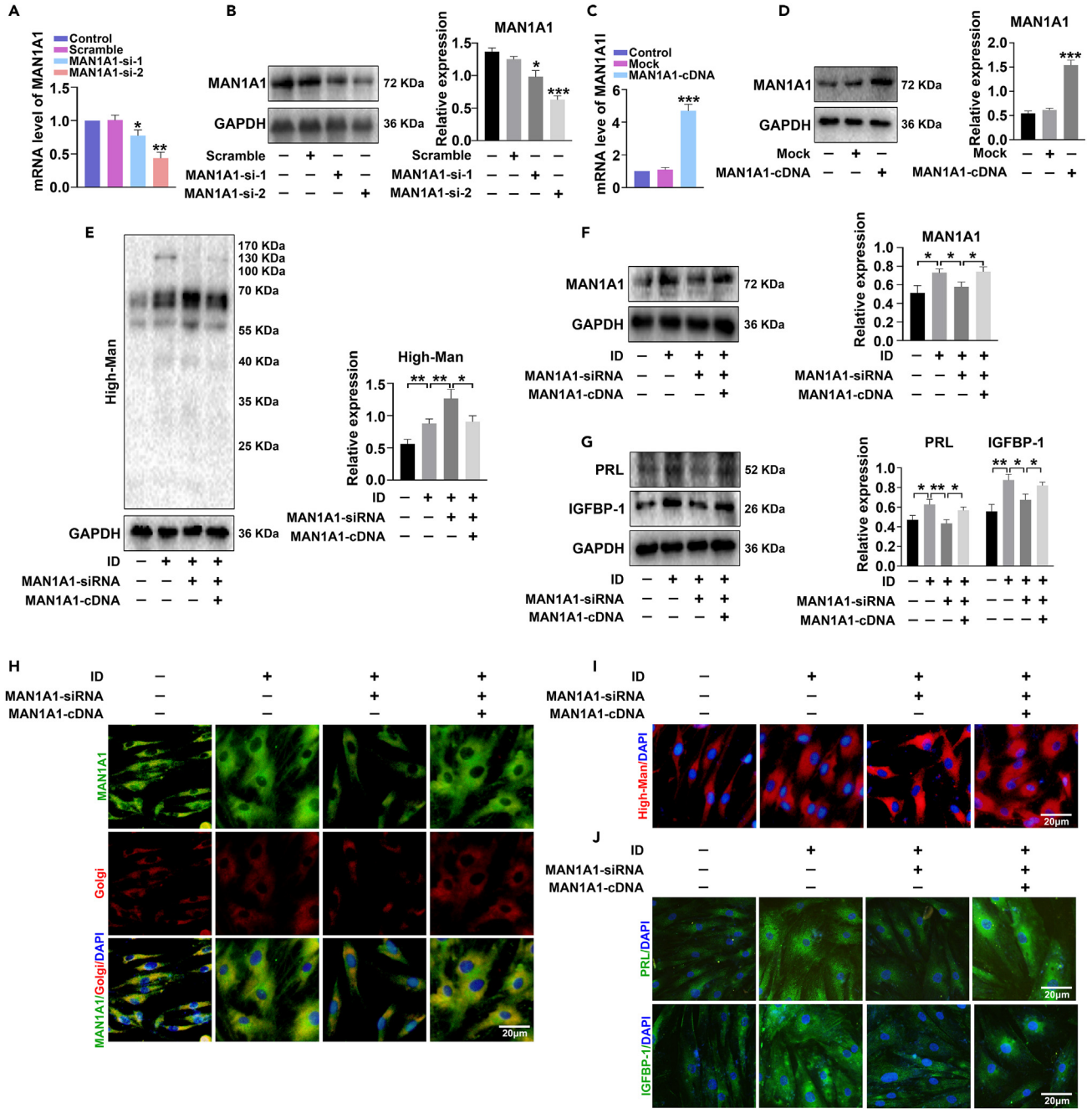

Figure 2. Silencing MAN1A1 increases high-mannose synthesis and inhibits decidualization of endometrial stromal cells

(A–D) HESCs were transfected with MAN1A1-siRNA and MAN1A1-cDNA, and mRNA and protein levels of MAN1A1 were detected by qPCR and western blot. (E–G) Western blot analysis of MAN1A1, PRL (prolactin), and insulin-like growth factor-binding protein 1 (IGFBP-1) expression and Lectin blot analysis of high-mannose expression in HESCs after artificial decidua induction (ID) with MPA and dbcAMP, followed by transfection with MAN1A1-siRNA and MAN1A1-cDNA. (H–J) Immunofluorescent staining of MAN1A1 (green), high-mannose (red), decidualization markers PRL (green), and IGFBP-1 (green) in HESCs after ID or uninduced control, followed by transfection with MAN1A1-siRNA or cotransfection with MAN1A1-cDNA. Golgi apparatus was labeled by Golgi-Tracker Red. Nuclei were stained with DAPI (blue). Scale bars, 20 μm *p < 0.05, **p < 0.01, ***p < 0.001.

enriched by Gene Ontology (GO) analysis (Figure 3C). Among them, lncNEAT1 and lncPCA3 were upregulated in infertile patients and associated with decidualization-related proliferation. Moreover, the organizational location analysis by the lncSEA database (http://bio.liclab.net/LncSEAv1/) indicated that lncNEAT1 was expressed in many organs, including uterus (Figure 3D). Herein, lncNEAT1 was identified as an essential candidate regulating MAN1A1 expression for subsequent study.

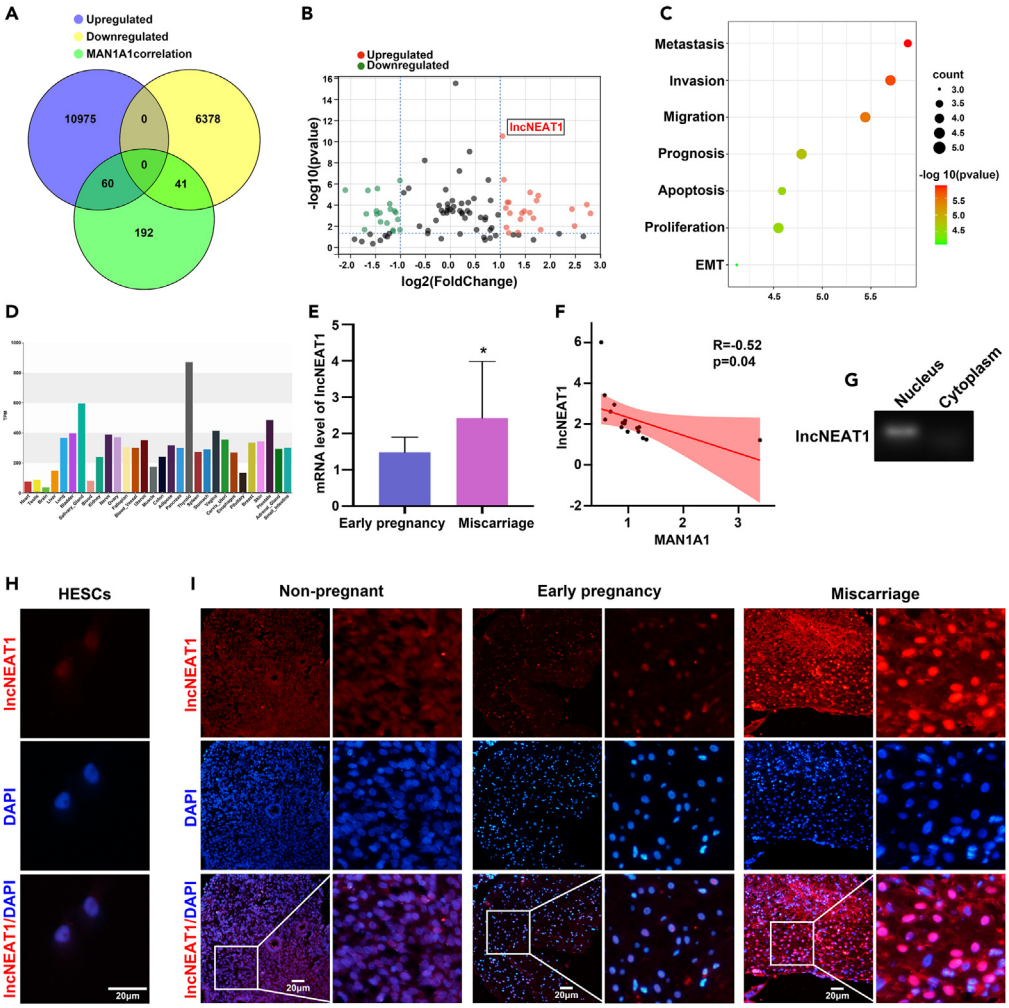

Figure 3. Increased lncNEAT1 level in the decidual tissues of miscarriage patients

(A) Integrative analysis of upregulated and downregulated lncRNAs in the serum of infertile patients compared with healthy women, and MAN1A1-correlated lncRNAs by Venn diagram.

(B) Intersection of lncRNAs (fold change >2) in correlation with MAN1A1 by volcano plot. lncNEAT1: para-nuclear assembled transcript 1.

(C) GO enrichment graph for upregulated lncRNAs by LncSEA database.

(D) Expression and localization of lncNEAT1 in human tissues by LncSEA database.

(E) qPCR analysis of lncNEAT1 level in the decidual tissues of early pregnancy and miscarriage.

(F) Pearson correlation analysis of lncNEAT1 and MAN1A1. Pearson R = 0.52; p = 0.04; n = 16. Linear regression: $y = -0.2274x + 1.633$; $r^2 = 0.2604$.

(G) lncNEAT1 level in the nucleus and cytoplasm of HESCs by PCR.

(H and I) Fluorescence *in situ* hybridization (FISH) analysis of lncNEAT1 (red) in HESCs (H) and endometrial tissues (I). Nuclei are stained with DAPI (blue). Scale bars, 20 μm *p < 0.05.

Furthermore, qPCR detection confirmed that lncNEAT1 level in miscarriage decidual tissues was higher than that in early pregnant tissues, and negatively correlated with MAN1A1 level (Figures 3E and 3F). FISH (Fluorescence *in situ* hybridization) results confirmed that lncNEAT1 was mainly located in the nucleus of HESCs (Figure 3H). Meanwhile, subcellular localization results showed that lncNEAT1 was mainly present in the nucleus but not the cytoplasm (Figure 3G). Furthermore, compared with non-pregnant endometrial tissue, lncNEAT1 expression was decreased in early pregnant endometrial tissues, and lncNEAT1 level was significantly increased in endometrial tissue of miscarriage patients compared with early pregnant group (Figure 3I).

lncNEAT1 hampered decidualization of endometrial stromal cells by decreasing MAN1A1 expression

The relationship between lncNEAT1 and MAN1A1 and their roles in decidualization were analyzed *in vitro*. The lncNEAT1 level was decreased or increased after transfection with lncNEAT1-siRNA or lncNEAT1-cDNA in HESCs (Figures 4A and 4B). Then the effect of lncNEAT1 on HESCs decidualization was detected; the data showed that lncNEAT1-siRNA transfection increased PRL and IGFBP-1 expression (Figures 4G and

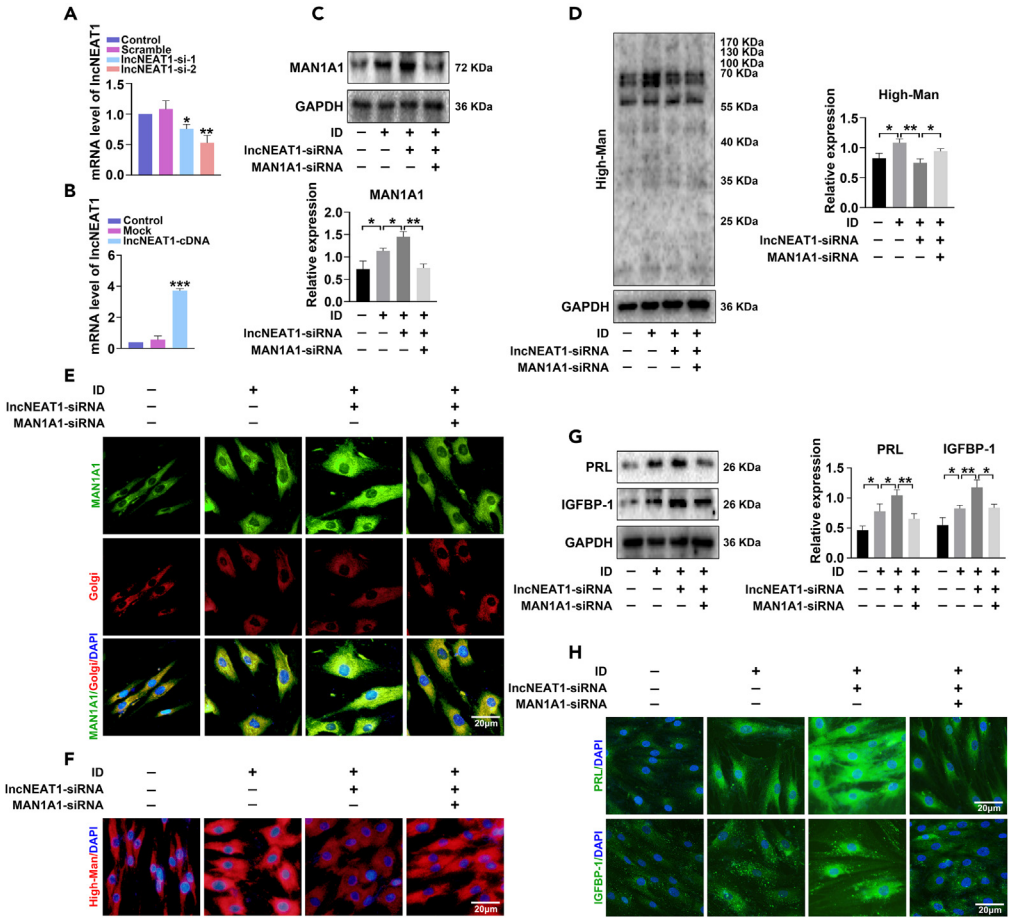

Figure 4. lncNEAT1 hampered decidualization of endometrial stromal cells by decreasing MAN1A1 expression

(A and B) qPCR analysis of lncNEAT1 level in HESCs after transfection with lncNEAT1-siRNA or lncNEAT1-cDNA.

(C, D, and G) Western blot analysis of MAN1A1, PRL, and IGFBP-1 expression and Lectin blot analysis of high-mannose in HESCs after ID, and transfection with lncNEAT1-siRNA or cotransfection with MAN1A1-siRNA.

(E, F, and H) Immunofluorescent staining of MAN1A1 (green), high-mannose (red), PRL (green), and IGFBP-1 (green) in HESCs after ID, and transfection with lncNEAT1-siRNA or cotransfection with MAN1A1-siRNA. Golgi apparatus was labeled by Golgi-Tracker Red. Nuclei are stained with DAPI (blue). Scale bars, 20 μm *$p < 0.05$, **$p < 0.01$.

4H). We subsequently explored the regulatory effect of lncNEAT1 on MAN1A1 expression in decidualization. Downregulation of lncNEAT1 increased MAN1A1 expression (Figures 4C and 4E) and inhibited high-mannose biosynthesis (Figures 4D and 4F). However, cotransfection with MAN1A1-siRNA attenuated the effect of lncNEAT1 compared with lncNEAT1-siRNA transfection group. Immunofluorescent staining showed more obviously decidual change of HESCs, such as cellular polygons and enlargement, as well as multiple nuclei after decidua induction. The less decidual change of HESCs was observed in transfection with lncNEAT1-siRNA, while it was recovered in cotransfection with MAN1A1-siRNA (Figures 4E, 4F, and 4H).

lncNEAT1 and MAN1A1 affect embryo implantation by decreasing decidualization *in vivo*

The roles of lncNEAT1 and MAN1A1 in decidualization were explored *in vivo*. Firstly, we detected lncNEAT1 and MAN1A1 levels in the non-pregnant mouse endometrium of estrus and diestrus phases, which is equivalent to those of human endometrium in secretory and proliferative phases. Immunofluorescent staining and FISH results showed that MAN1A1 expression was increased; lncNEAT1 expression and high-mannose biosynthesis were decreased in diestrus phase compared with those in estrus phase (Figures S7A and S7B). The pregnant mice on GD 3 (time point for embryo implantation) were randomly divided into two groups, and injected into one side of uterine horns with normal saline (control), and another side with lncNEAT1-cDNA in group 1. Similarly, lncNEAT1-cDNA and lncNEAT1-cDNA + MAN1A1-cDNA were injected into either of the uterine horns in group 2. Mice were sacrificed, and uterus was collected on GD 7 (time point for decidualization) (Figure 5A). The results showed that embryo implantation rate was significantly reduced in lncNEAT1-cDNA injection compared with control (9 ± 2 *vs.* 4 ± 2) (Figure 5B), while implantation rate was increased in lncNEAT1-cDNA + MAN1A1-cDNA injection compared with lncNEAT1-cDNA

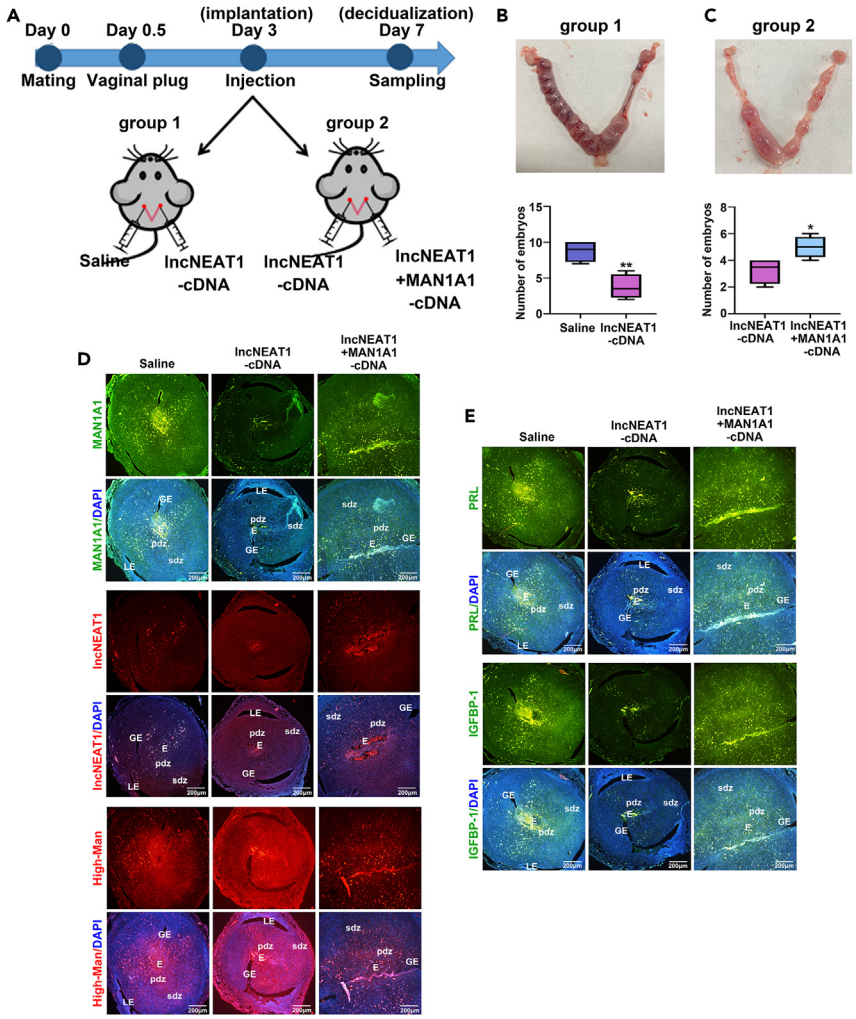

Figure 5. lncNEAT1 and MAN1A1 affect embryo implantation by decreasing decidualization *in vivo*

(A) Schematic diagram of mouse pregnant model plan.

(B and C) Number of embryos implanted at GD 7 in group 1 injected normal saline (control) and lncNEAT1-cDNA, and group 2 injected lncNEAT1-cDNA and lncNEAT1-cDNA + MAN1A1-cDNA.

(D and E) Immunofluorescent staining of MAN1A1 (green), lncNEAT1 (red), high-mannose (red), PRL (green), and IGFBP-1 (green) in the uterus of GD 7. Nuclei are stained with DAPI (blue). Scale bars, 200 μm. LE: luminal epithelium; GE: glandular epithelium; E: embryo; pdz: primary decidual zone; sdz: secondary decidual zone. *p < 0.05, **p < 0.01.

injection (3 ± 1 *vs.* 5 ± 2) (Figure 5C). Immunofluorescent staining showed that MAN1A1 expression was decreased; lncNEAT1 expression and high-mannose biosynthesis were increased in control compared with lncNEAT1-cDNA injection. However, MAN1A1 expression was recovered; lncNEAT1 expression and high-mannose biosynthesis were reduced in lncNEAT1-cDNA + MAN1A1-cDNA injection compared with lncNEAT1-cDNA injection (Figures 5D and 5E). In addition, the embryo implantation sites were obvious and the decidualization reaction in pdz (primary decidual zone) and sdz (secondary decidual zone) was clear in control endometrium. Compared with control, the diameter of implantation sites was reduced; pdz and sdz were reduced significantly in lncNEAT1-cDNA. The decidualization was evident in lncNEAT1-cDNA + MAN1A1-cDNA compared with lncNEAT1-cDNA (Figures 5D and 5E). Taken together, the results indicated that the increased lncNEAT1 led to the loss of endometrial decidualization by inhibiting MAN1A1 expression, which may be related to abortion and infertility.

Binding of lncNEAT1 and NPM1-SP1 complex inhibits MAN1A1 transcription

Having observed the functions of lncNEAT1 and MAN1A1 on decidualization and embryo implantation *in vitro* and *in vivo*, the underlying molecular mechanisms were further verified. Here, lncNEAT1 pull-down was used to obtain the proteins binding with lncNEAT1 from uninduced and decidua-induced HESCs. The collected proteins were identified by liquid chromatography-tandem mass spectrometry (LC-MS/MS) (Figure 6A). Totally, 617 proteins interacting with lncNEAT1 were identified in HESCs, and 347 upregulated proteins included

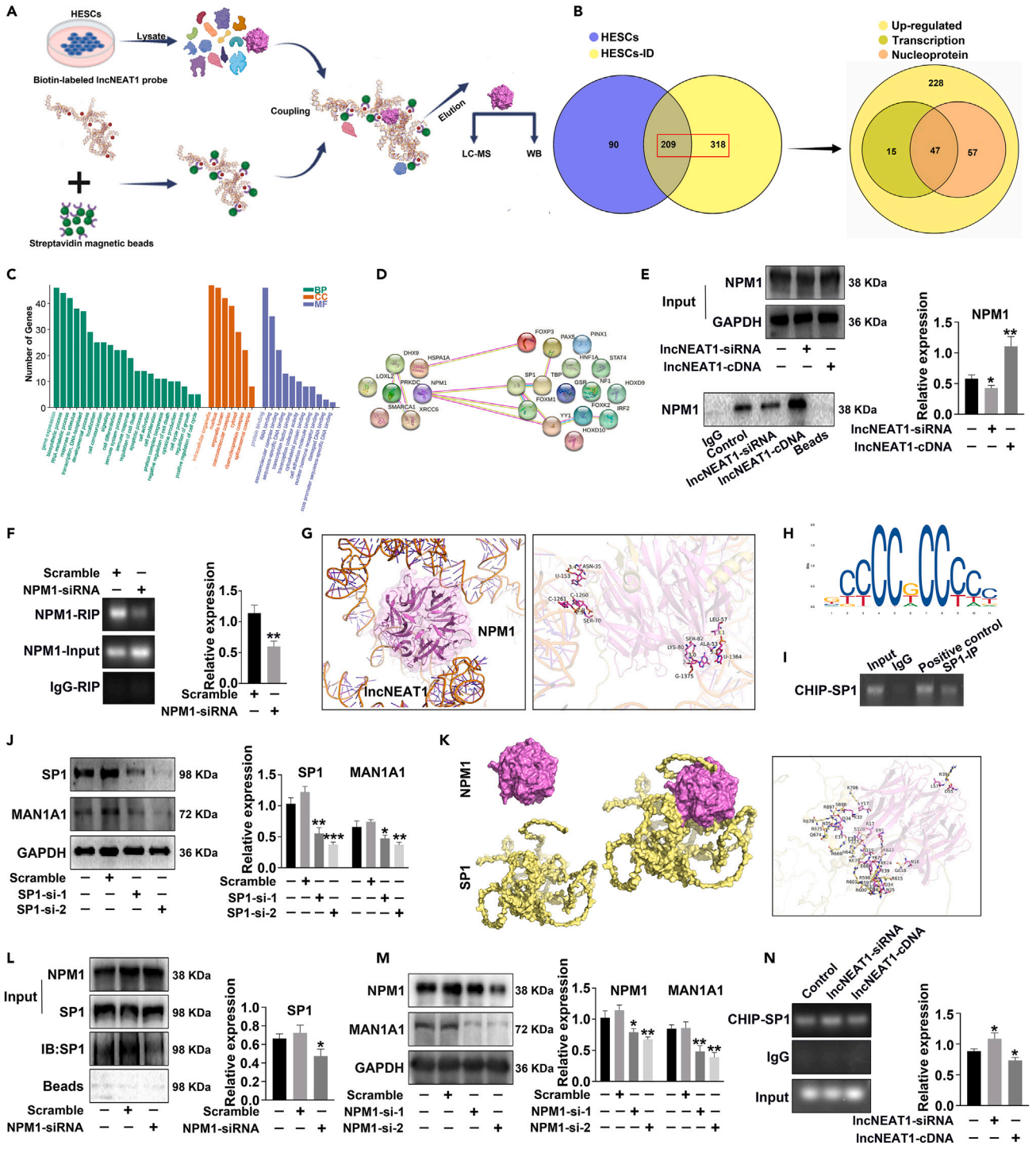

Figure 6. Binding of lncNEAT1 and NPM1-SP1 complex inhibits MAN1A1 transcription

(A) Schematic summary of biotin-labeled lncNEAT1 pull-down protocol.

(B) LC-MS/MS analysis of lncNEAT1 binding proteins by Venn diagram: lncNEAT1 pull-down protein in HESCs and HESCs-ID (left); transcription-associated proteins and nuclear proteins in upregulated HESCs-ID (right).

(C) GO analysis of 47 intersecting proteins.

(D) Protein-protein interaction network analysis of lncNEAT1-binding proteins associated with decidualization and transcription factors of MAN1A1 by STRING database.

(E) lncNEAT1 pull-down analysis of NPM1 (nucleophosmin) expression in HESCs after transfection with lncNEAT1-siRNA or lncNEAT1-cDNA.

Figure 6. *Continued*

(F) RIP (RNA-binding protein immunoprecipitation) analysis of lncNEAT1 levels in HESCs after transfection with NPM1-siRNA.

(G) Demonstration of molecular docking of lncNEAT1 and NPM1. Yellow dashed line: hydrogen bonds.

(H) SP1 binding motif sequence logo from JASPAR database.

(I) ChIP (Chromatin immunoprecipitation) analysis of the binding site between SP1 and the promoter of MAN1A1.

(J and M) Western blot analysis of MAN1A1 expression in HESCs after transfection with SP1-siRNA or NPM1-siRNA.

(K) Molecular docking of NPM1 and SP1. Yellow dashed line: hydrogen bonds; pink dashed line: salt bridges.

(L) Immunoprecipitation analysis of NPM1 and SP1 in HESCs transfected with scramble or NPM1 siRNA. IP: protein pulled down with an anti-NPM1 antibody. IB: detection of SP1 expression by antibody.

(N) ChIP analysis of SP1 and the MAN1A1 promoter binding in HESCs after transfection with lncNEAT1-siRNA and lncNEAT1-cDNA. *$p < 0.05$, **$p < 0.01$, ***$p < 0.001$.

62 transcription-related proteins and 104 nuclear expression proteins in decidua-induced HESCs. The aforementioned 47 proteins located in nucleus were involved in transcription process (Figure 6B). GO analysis showed they were involved in various biological processes including cell communication, development, signaling, differentiation, proliferation, and adhesion (Figure 6C). Based on the proliferation and differentiation traits in decidualization, 7 proliferation- and differentiation-related proteins (NPM1, LOXL2, SMARCA1, PRKDC, XRCC6, HSPA1A, and DHX9) were selected for further investigation.

To find the specific transcription factors binding to the promoter of MAN1A1, 16 potential target transcription factors were selected by PROMO website (http://alggen.lsi.upc.es/cgi-bin/promo/). Protein-protein interactions were analyzed between 7 lncNEAT1 binding proteins and 16 transcription factors by STRING database (https://string-db.org/), and only NPM1 (nucleophosmin) could interact with multiple transcription factors of MAN1A1 (Figure 6D). Subsequently, lncNEAT1 pull-down and western blot results confirmed that lncNEAT1 stably interacted with NPM1. lncNEAT1-siRNA and lncNEAT1-cDNA decreased and increased the binding ability between lncNEAT1 and NPM1, respectively (Figure 6E). Accordingly, RNA-binding protein immunoprecipitation verified the combination of lncNEAT1 and NPM1, and silencing NPM1 by specific siRNA repressed the binding of NPM1 and lncNEAT1 (Figure 6F). The molecular docking data (http://hdock.phys.hust.edu.cn/) predicted the binding site of lncNEAT1 and NPM1 (PDB ID: 5EHD) at RNA sites U152, C1260, C1261, U1364, and G1375 and protein sites Asn35, Ser70, Ala53, Leu57, Lys82, and Ser80 according to the PDB database and HDOCK server using PyMOL and AutoDockTools software (Figure 6G).

We subsequently explored how lncNEAT1 and NPM1 regulate MAN1A1 expression. Among the multiple transcription factors of MAN1A1, SP1 was the highest confidence factor based on JASPAR database (https://jaspar.genereg.net/), and the motif of binding site was shown in Figure 6H. Chromatin immunoprecipitation confirmed the binding of SP1 and promoter of MAN1A1 (Figure 6I). Moreover, SP1 downregulation by SP1-siRNA transcription correspondingly inhibited the expression of MAN1A1 (Figure 6J). The molecular docking data showed that there were three evolutionarily conserved acidic residues (Asp36, Glu39, and Glu93) in NPM1 which could bind to target proteins containing R-rich motifs to stabilize NPM1 form. SP1 is rich in arginine at (^{597}**RR**T**RR**EACTCPYCKDSEG**R**^{615}), suggesting that NPM1 and SP1 likely form stable complex (Figure 6K). In addition, immunoprecipitation by NPM1 antibody showed that downregulating NPM1 expression by NPM1-siRNA did not affect SP1 expression but decreased the interaction of NPM1 and SP1 (Figure 6L). Moreover, silencing NPM1 downregulated MAN1A1 expression by western blot (Figure 6M). lncNEAT1-siRNA promoted and lncNEAT1-cDNA inhibited the binding of NPM1/SP1 to the promoter of MAN1A1 (Figure 6N). The aforementioned results provided evidence that NPM1 and SP1 could form a complex that facilitated the transcription of MAN1A1.

DISCUSSION

Glycobiology of reproduction reveals that protein glycosylation plays an important role in the regulation of reproductive functions. The stage-specific changes in glycoproteins and glycans, as well as the corresponding glycoenzymes, support endometrial decidualization. Here, we provided evidence of higher level of high-mannose glycans, and lower expression of MAN1A1 in the decidua of miscarriage patients exerted inhibitory effect on endometrial decidualization both in human stromal cells and mouse pregnant model. Moreover, mechanistic studies also demonstrated that increased lncNEAT1 level enhanced its binding ability with NPM1-SP1 complex, resulting in weakened combination of the complex at the promoter, thus inhibiting MAN1A1 transcription and hampering endometrial decidualization.

The accumulated data indicate the specific glycans of scaffold proteins present on the surface of endometrial epithelium, stroma, and embryonic trophoblast.[28] Exometabolomic analysis found that the levels of glucosylsphingosine and hyaluronic acid were increased, while the level of lactosamine was decreased in endometrial stromal cells after decidua induction.[29] Sialic acid is involved in the development of endometriosis by promoting migration and invasion of endometrial cells.[30,31] In addition, abnormal glycosylation leads to the occurrence and development of pregnancy-related diseases, such as premature delivery, preeclampsia, intrauterine growth restriction, and placental abruption.[32–36] In the current study, employing Lectin microarray, we screened and identified high-mannose glycoforms present at higher levels in decidua of miscarriage patients than that in healthy early pregnant controls. Lectins BANLEC and GRFT recognize α1,2-terminated glycans. According to Lectin microarray, increased BANLEC and decreased GRFT trend was found, but the difference was not statistically significant. GNA showed good uniformity in early pregnant women and miscarriage patients. Herein, GNA was used as the candidate. The expression trait and function of glycans recognized by BANLEC and GRFT need further exploration. Hyun et al. reported that high-mannose glycans were not commonly presented on the surfaces of mammalian cells or in serum, yet may play important roles in stem cell biology.[37] Decidualization is a differentiation process of stromal cells involving morphological and secretory function changes. We hypothesized that high-mannose

glycans participated in the initiation of endometrial decidualization. Employing a decidua-induced system *in vitro*, we provide evidence that a higher level of high-mannose blunts decidualization of stromal cells. Gary et al. found the uterus was highly enriched in glycoconjugates which were associated with the secretions released by epithelial and stromal cells.[38] Complex glycan epitopes play essential roles in decidualization, and evidence suggests that altering the structural nature of N-glycans may impact trophoblast function, including those related to interactions with decidual cells.[39] During glycosylation processing, high-mannose is the basis of complex and hybrid N-glycans biosynthesis. Here, we checked the complex glycans by Lectin blot with PHA-E+L. The results showed that complex glycans were decreased after MAN1A1-siRNA transfection, and increased after MAN1A1-cDNA transfection (Figure S6). It suggested that the N-glycosylation pathway was blocked at high-mannose stage, and a substantial reduction in complex glycans, which can carry important functional epitopes. Furthermore, Montacir et al. reported that high-mannose N-glycans were the main components of surface glycosylation in the undifferentiated embryonic stem cells. The decreased high-mannose and increased complex N-glycans were observed in differentiated embryonic stem cells,[40] indicating the accompanied decreased high-mannose and increased complex N-glycans in the differentiation. Endometrial decidualization is also a differentiation process, and the specific glycoproteins modified by complex N-glycans need further study.

Increased levels/activities of ALGs or decreased levels of MANs accumulate the high-mannose content, further mediating physiological and pathological processes. For example, ALG2 expression is inhibited in silver-nanocolloids-exposed embryos, resulting in reduced high-mannose synthesis.[41] In the current study, we screened enzymes and found that MAN1A1 level was decreased significantly in the decidua of miscarriage patients compared with early pregnant women. MAN1A1 participates in glycan biosynthesis by hydrolyzing α1,2-mannose in the maturation of N-glycans in Golgi apparatus. In the absence of MAN1A1, N-glycans arrest in the high-mannose form, whereas in the presence of MAN1A1, mannose residues are cleaved and replaced by glucose, fucose, and sialic acid, producing highly variable complex N-glycans.[42] There have been few studies on MAN1A1 in reproduction. Here, our results demonstrated that silencing MAN1A1 led to the accumulation of high-mannose N-glycans in endometrial stromal cells, prevented cells from differentiating into decidual cells, and ultimately resulted in endometrial receptivity formation failure. Although we only studied MAN1A1 according to the screening results, it is not "special", and other mannosidases may be also involved in decidualization based on the complex expression and function traits of glycoenzymes.

LncRNAs regulated gene expression at the transcriptional level, thus influencing the corresponding biological processes. Increasing evidence has shown that lncRNAs play important roles in pregnancy. Reports have shown that lncMALT1, lncHELLP, and lncPRNCR1 mediate mouse embryo development, invasion, and sex determination, respectively.[43–45] Here, employing RNA sequencing and bioinformatics analysis, we globally screened and compared lncRNAs from early pregnant women and miscarriage patients. Our results showed that lncNEAT1 was significantly elevated in the decidua of miscarriage, and there was a negative regulatory relationship between lncNEAT1 and MAN1A1. Although lncNEAT1 has been reported to be increased in cancer, it is seldom studied in reproduction. It was found that lncNEAT1 level was enhanced in the placental tissues of preeclampsia rats, which accelerated apoptosis and inhibited proliferation, invasion, and migration of trophoblast cells.[46] Here, we explored the expression trait and function of lncNEAT1 in decidualization. The results showed that upregulation of lncNEAT1 inhibited MAN1A1 expression and hampered decidualization both *in vitro* and *in vivo*. Based on differential expression and functions of lncRNAs in physiological and pathological processes, lncRNAs are potential biomarkers for diagnostic and therapeutic targets. The high level of lncTCL6 in the placenta and peripheral blood served as the diagnostic biomarkers for preeclampsia.[47] In this study, we found elevated lncNEAT1 level in the serum and endometrial tissue of miscarriage patients. Furthermore, upregulating lncNEAT1 level facilitated decidualization which was associated with functional receptivity of embryos. The results suggest that lncNEAT1 is a potential biomarker for diagnosis of aberrant decidualization and therapeutic intervention of miscarriage.

The molecular mechanism of lncNEAT1 includes interacting with microRNA, histone protease, transcription factors, mRNA, and so on. For example, lncNEAT1 promoted M2 macrophage polarization and choroidal neovascularization by targeting PTEN via miR-148a-3p.[48] Abnormally high expression of lncNEAT1 synergistically interacts with EZH2 to promote invasion and metastasis of gastric cancer cells.[49] lncNEAT1 activates the transcriptional activity of β-catenin by binding DDX5, and then promotes progression/metastasis of colorectal cancer.[50] Brighton et al. reported that increased transcription factor FOXO1 in the stromal cells promoted decidual-like differentiation and facilitated embryo implantation.[51] In this study, lncNEAT1 pull-down and LC-MS/MS analysis were performed to identify the protein molecules bound to lncNEAT1. The results showed that lncNEAT1 interacted with many proteins, especially transcription factors and transcription-related factors. We assumed that these factors participated in the regulation of MAN1A1 gene expression. Hence, through GO enrichment analysis and transcription factor prediction, the lncNEAT1-binding protein NPM1 was screened out, and it could interact with SP1, a transcription factor of MAN1A1. Immunoprecipitation results confirmed the regulatory effect of NPM1-SP1 transcription complex on MAN1A1 expression. It was found that NPM1 acted as a partner of the nuclear factor κB transcription complex, and enhanced MnSOD transcription.[52] The function of NPM1-SP1 transcription complex in gene expression remains unclear. Here, we proposed and confirmed that the lncNEAT1/NPM1/SP1 axis regulated MAN1A1 promoter activity and transcription.

In summary, the abnormal elevation of high-mannose N-glycans had an adverse effect on endometrial decidualization, and MAN1A1 degrading high-mannose was regulated by lncNEAT1, which controlled the transcription of MAN1A1 through NPM1-SP1 transcription complex. This study suggests the glycobiological mechanism of miscarriage pathogenesis and provides new ideas to improve endometrial receptivity for successful pregnancy.

Limitations of the study

This study mainly explored the role of high-mannose N-glycans during endometrial decidualization. The results revealed that elevated high-mannose N-glycans by reduced mannosidase MAN1A1 expression hampered endometrial decidualization. Furthermore, MAN1A1

transcription was regulated by lncNEAT1 and NPM1-SP1 complex. Except MAN1A1, we also found that other MANs and ALGs were differently expressed in the decidua of miscarriage and normal pregnancy. Subsequent studies will define whether these enzymes were involved in the decidualization.

STAR★METHODS

Detailed methods are provided in the online version of this paper and include the following:

- KEY RESOURCES TABLE
- RESOURCE AVAILABILITY
  - Lead contact
  - Materials availability
  - Data and code availability
- EXPERIMENTAL MODEL AND STUDY PARTICIPANT DETAILS
  - Human specimens
  - Cell lines
  - Animal experiments
- METHOD DETAILS
  - Lectin microarray
  - Cell transfection
  - RNA extraction and quantitative PCR (qPCR)
  - Western blot
  - Immunohistochemistry
  - Immunofluorescence
  - RNA pull-down
  - Immunoprecipitation
  - RNA-binding protein immunoprecipitation (RIP)
  - Chromatin immunoprecipitation (ChIP)
  - Subcellular fractionation location
  - Fluorescence *in situ* hybridization (FISH)
- QUANTIFICATION AND STATISTICAL ANALYSIS

SUPPLEMENTAL INFORMATION

Supplemental information can be found online at https://doi.org/10.1016/j.isci.2023.108170.

ACKNOWLEDGMENTS

This work was supported by Liaoning Provincial Program for Top Discipline of Basic Medical Sciences.

AUTHOR CONTRIBUTIONS

S.L. and Q.Y. designed the experiments. S.C., A.Z., and N.L. performed the experiments. S.C., A.Z., H.W., and Y.L. analyzed the data. S.C., S.L., and Q.Y. edited the manuscript.

DECLARATION OF INTERESTS

The authors declare no competing interests.

Received: January 20, 2023
Revised: April 17, 2023
Accepted: October 6, 2023
Published: October 14, 2023

REFERENCES

1. Lidegaard, Ø., Mikkelsen, A.P., Egerup, P., Kolte, A.M., Rasmussen, S.C., and Nielsen, H.S. (2020). Pregnancy loss: A 40-year nationwide assessment. Acta Obstet. Gynecol. Scand. *99*, 1492–1496.
2. Ramhorst, R., Grasso, E., Vota, D., Gori, S., Hauk, V., Paparini, D., Calo, G., and Pérez Leirós, C. (2022). From decidualization to pregnancy progression: An overview of immune and metabolic effects of VIP. Am. J. Reprod. Immunol. *88*, e13601.
3. Ochoa-Bernal, M.A., and Fazleabas, A.T. (2020). Physiologic events of embryo implantation and decidualization in human and non-human primates. Int. J. Mol. Sci. *21*, 1973.
4. Wu, J., Lin, S., Huang, P., Qiu, L., Jiang, Y., Zhang, Y., Meng, N., Meng, M., Wang, L., Deng, W., et al. (2022). Maternal anxiety affects embryo implantation via impairing adrenergic receptor

signaling in decidual cells. Commun. Biol. *5*, 840.

5. Yoshie, M., Kusama, K., Tanaka, R., Okubo, T., Kojima, J., Takaesu, Y., Isaka, K., Nishi, H., and Tamura, K. (2021). Possible roles of calreticulin in uterine decidualization and receptivity in rats and humans. Int. J. Mol. Sci. *22*, 10505.
6. Wang, X.B., Qi, Q.R., Wu, K.L., and Xie, Q.Z. (2018). Role of osteopontin in decidualization and pregnancy success. Reproduction *155*, 423–432.
7. Al-Sabbagh, M., Fusi, L., Higham, J., Lee, Y., Lei, K., Hanyaloglu, A.C., Lam, E.W.F., Christian, M., and Brosens, J.J. (2011). NADPH oxidase-derived reactive oxygen species mediate decidualization of human endometrial stromal cells in response to cyclic AMP signaling. Endocrinology *152*, 730–740.
8. Shao, Q., Liu, X., Huang, Y., Chen, X., and Wang, H. (2020). Human decidual stromal cells in early pregnancy induce functional re-programming of monocyte-derived dendritic cells via crosstalk between G-CSF and IL-1. Front. Immunol. *11*, 574270.
9. Huang, P., Deng, W., Bao, H., Lin, Z., Liu, M., Wu, J., Zhou, X., Qiao, M., Yang, Y., Cai, H., et al. (2022). SOX4 facilitates PGR protein stability and FOXO1 expression conducive for human endometrial decidualization. Elife *11*, e72073.
10. Kakita-Kobayashi, M., Murata, H., Nishigaki, A., Hashimoto, Y., Komiya, S., Tsubokura, H., Kido, T., Kida, N., Tsuzuki-Nakao, T., Matsuo, Y., et al. (2020). Thyroid hormone facilitates *in vitro* decidualization of human endometrial stromal cells via thyroid hormone receptors. Endocrinology *161*, bqaa049.
11. Fuster, M.M., and Esko, J.D. (2005). The sweet and sour of cancer: Glycans as novel therapeutic targets. Nat. Rev. Cancer *5*, 526–542.
12. Boune, S., Hu, P., Epstein, A.L., and Khawli, L.A. (2020). Principles of N-Linked glycosylation variations of IgG-based therapeutics: pharmacokinetic and functional considerations. Antibodies *9*, 22.
13. Bordron, A., Morel, M., Bagacean, C., Dueymes, M., Pochard, P., Harduin-Lepers, A., Jamin, C., and Pers, J.O. (2021). Hyposialylation must be considered to develop future therapies in autoimmune diseases. Int. J. Mol. Sci. *22*, 3402.
14. Mun, G.I., Lee, S.J., An, S.M., Kim, I.K., and Boo, Y.C. (2009). Differential gene expression in young and senescent endothelial cells under static and laminar shear stress conditions. Free Radic. Biol. Med. *47*, 291–299.
15. Lee, J.T. (2012). Epigenetic regulation by long noncoding RNAs. Science *338*, 1435–1439.
16. Kim, T.K., Hemberg, M., and Gray, J.M. (2015). Enhancer RNAs: A class of long noncoding RNAs synthesized at enhancers. Cold Spring Harb. Perspect. Biol. *7*, a018622.
17. Guennewig, B., and Cooper, A.A. (2014). The central role of noncoding RNA in the brain. Int. Rev. Neurobiol. *116*, 153–194.
18. Prudhomme, J., and Morey, C. (2016). Epigenesis and plasticity of mouse trophoblast stem cells. Cell. Mol. Life Sci. *73*, 757–774.
19. Schmitz, S.U., Grote, P., and Herrmann, B.G. (2016). Mechanisms of long noncoding RNA function in development and disease. Cell. Mol. Life Sci. *73*, 2491–2509.
20. Zhang, Q., Wang, Z., Cheng, X., and Wu, H. (2021). lncRNA DANCR promotes the migration an invasion and of trophoblast cells through microRNA-214-5p in preeclampsia. Bioengineered *12*, 9424–9434.
21. Sheng, F., Sun, N., Ji, Y., Ma, Y., Ding, H., Zhang, Q., Yang, F., and Li, W. (2019). Aberrant expression of imprinted lncRNA MEG8 causes trophoblast dysfunction and abortion. J. Cell. Biochem. *120*, 17378–17390.
22. Liu, L.P., and Gong, Y.B. (2018). LncRNA-TCL6 promotes early abortion and inhibits placenta implantation via the EGFR pathway. Eur. Rev. Med. Pharmacol. Sci. *22*, 7105–7112.
23. Zeng, H., Fan, X., and Liu, N. (2017). Expression of H19 imprinted gene in patients with repeated implantation failure during the window of implantation. Arch. Gynecol. Obstet. *296*, 835–839.
24. Wang, Y., Hu, S., Yao, G., Zhu, Q., He, Y., Lu, Y., Qi, J., Xu, R., Ding, Y., Li, J., et al. (2020). A novel molecule in human cyclic endometrium: LncRNA TUNAR is involved in embryo implantation. Front. Physiol. *11*, 587448.
25. Xu, Z., Jin, H., Duan, X., Liu, H., Zhao, X., Fan, S., Wang, Y., and Yao, T. (2021). LncRNA PSMA3-AS1 promotes cell proliferation, migration, and invasion in ovarian cancer by activating the PI3K/Akt pathway via the miR-378a-3p/GALNT3 axis. Environ. Toxicol. *36*, 2562–2577.
26. Fan, X., Lou, J., Zheng, X., Wang, Y., Wang, J., Luo, M., and Hu, M. (2021). Interference with lncRNA NEAT1 promotes the proliferation, migration, and invasion of trophoblasts by upregulating miR-411-5p and inhibiting PTEN expression. Immunopharmacol. Immunotoxicol. *43*, 334–342.
27. Xiang, Y., Karaveg, K., and Moremen, K.W. (2016). Substrate recognition and catalysis by GH47 α-mannosidases involved in Asn-linked glycan maturation in the mammalian secretory pathway. Proc. Natl. Acad. Sci. USA *113*, E7890–E7899.
28. Jones, C.J.P., and Aplin, J.D. (2009). Glycosylation at the fetomaternal interface: Does the glycocode play a critical role in implantation? Glycoconj. J. *26*, 359–366.
29. Harden, S.L., Zhou, J., Gharanei, S., Diniz-da-Costa, M., Lucas, E.S., Cui, L., Murakami, K., Fang, J., Chen, Q., Brosens, J.J., and Lee, Y.H. (2021). Exometabolomic analysis of decidualizing human endometrial stromal and perivascular cells. Front. Cell Dev. Biol. *9*, 626619.
30. Maignien, C., Santulli, P., Chouzenoux, S., Gonzalez-Foruria, I., Marcellin, L., Doridot, L., Jeljeli, M., Grange, P., Reis, F.M., Chapron, C., and Batteux, F. (2019). Reduced α-2,6 sialylation regulates cell migration in endometriosis. Hum. Reprod. *34*, 479–490.
31. Choi, H.J., Chung, T.W., Choi, H.J., Han, J.H., Choi, J.H., Kim, C.H., and Ha, K.T. (2018). Increased α2-6 sialylation of endometrial cells contributes to the development of endometriosis. Exp. Mol. Med. *50*, 1–12.
32. Goldenberg, R.L., Culhane, J.F., Iams, J.D., and Romero, R. (2008). Epidemiology and causes of preterm birth. Lancet *371*, 75–84.
33. Fretts, R.C. (2005). Etiology and prevention of stillbirth. Am. J. Obstet. Gynecol. *193*, 1923–1935.
34. Duley, L. (2009). The global impact of preeclampsia and eclampsia. Semin. Perinatol. *33*, 130–137.
35. Mercer, B.M. (2003). Preterm premature rupture of the membranes. Obstet. Gynecol. *101*, 178–193.
36. Romero, R., Dey, S.K., and Fisher, S.J. (2014). Preterm labor: One syndrome, many causes. Science *345*, 760–765.
37. An, H.J., Gip, P., Kim, J., Wu, S., Park, K.W., McVaugh, C.T., Schaffer, D.V., Bertozzi, C.R., and Lebrilla, C.B. (2012). Extensive determination of glycan heterogeneity reveals an unusual abundance of high mannose glycans in enriched plasma membranes of human embryonic stem cells. Mol. Cell. Proteomics *11*. M111.010660.
38. Clark, G.F. (2015). Functional glycosylation in the human and mammalian uterus. Fertil. Res. Pract. *1*, 17.
39. Huang, Z., Lai, P.F., Cocker, A.T.H., Haslam, S.M., Dell, A., Brady, H.J.M., and Johnson, M.R. (2023). Roles of N-linked glycosylation and glycan-binding proteins in placentation: trophoblast infiltration, immunomodulation, angiogenesis, and pathophysiology. Biochem. Soc. Trans. *51*, 639–653.
40. Montacir, H., Freyer, N., Knöspel, F., Urbaniak, T., Dedova, T., Berger, M., Damm, G., Tauber, R., Zeilinger, K., and Blanchard, V. (2017). The cell-surface N-glycome of human embryonic stem cells and differentiated hepatic cells thereof. Chembiochem *18*, 1234–1241.
41. Shimizu, K., Kotajima, D., Fukao, K., Mogi, F., Horiuchi, R., Kataoka, C., Kagami, Y., Fujita, M., Miyanishi, N., and Kashiwada, S. (2021). Exposure of silver nanocolloids causes glycosylation disorders and embryonic deformities in medaka. Toxicol. Appl. Pharmacol. *1*, 115714.
42. Moremen, K.W., Tiemeyer, M., and Nairn, A.V. (2012). Vertebrate protein glycosylation: diversity, synthesis and function. Nat. Rev. Mol. Cell Biol. *13*, 448–462.
43. Hamazaki, N., Uesaka, M., Nakashima, K., Agata, K., and Imamura, T. (2015). Gene activation-associated long noncoding RNAs function in mouse preimplantation development. Development *142*, 910–920.
44. Lv, J., Liu, H., Yu, S., Liu, H., Cui, W., Gao, Y., Zheng, T., Qin, G., Guo, J., Zeng, T., et al. (2015). Identification of 4438 novel lincRNAs involved in mouse preimplantation embryonic development. Mol. Genet. Genom. *290*, 685–697.
45. Taylor, D.H., Chu, E.T.J., Spektor, R., and Soloway, P.D. (2015). Long noncoding RNA regulation of reproduction and development. Mol. Reprod. Dev. *82*, 932–956.
46. Teng, L., Liu, P., Song, X., Wang, H., Sun, J., and Yin, Z. (2020). Long non-coding RNA nuclear-enriched abundant transcript1 (NEAT1) represses proliferation of trophoblast cells in rats with preeclampsia via the microRNA-373/FLT1 axis. Med. Sci. Monit. *26*, e927305.
47. He, X., He, Y., Xi, B., Zheng, J., Zeng, X., Cai, Q., Ouyang, Y., Wang, C., Zhou, X., Huang, H., et al. (2013). LncRNAs expression in preeclampsia placenta reveals the potential role of lncRNAs contributing to preeclampsia pathogenesis. PLoS One *8*, e81437.
48. Zhang, P., Lu, B., Zhang, Q., Xu, F., Zhang, R., Wang, C., Liu, Y., Wei, C., and Mei, L. (2020). LncRNA NEAT1 sponges miRNA-148a-3p to

suppress choroidal neovascularization and M2 macrophage polarization. Mol. Immunol. *127*, 212–222.

49. Zhang, J., Guo, S., Piao, H.Y., Wang, Y., Wu, Y., Meng, X.Y., Yang, D., Zheng, Z.C., and Zhao, Y. (2019). ALKBH5 promotes invasion and metastasis of gastric cancer by decreasing methylation of the lncRNA NEAT1. J. Physiol. Biochem. *75*, 379–389.

50. Zhang, M., Weng, W., Zhang, Q., Wu, Y., Ni, S., Tan, C., Xu, M., Sun, H., Liu, C., Wei, P., and Du, X. (2018). The lncRNA NEAT1 activates Wnt/β-catenin signaling and promotes colorectal cancer progression by interacting with DDX5. J. Hematol. Oncol. *11*, 113.

51. Brighton, P.J., Maruyama, Y., Fishwick, K., Vrljicak, P., Tewary, S., Fujihara, R., Muter, J., Lucas, E.S., Yamada, T., Woods, L., et al. (2017). Clearance of senescent decidual cells by uterine natural killer cells in cycling human endometrium. Elife *6*, e31274.

52. Dhar, S.K., Lynn, B.C., Daosukho, C., and St Clair, D.K. (2004). Identification of nucleophosmin as an NF-kappaB co-activator for the induction of the human SOD2 gene. J. Biol. Chem. *279*, 28209–28219.

STAR★METHODS

KEY RESOURCES TABLE

REAGENT or RESOURCE	SOURCE	IDENTIFIER
Antibodies		
Anti-IGFBP-1	Affinity	Cat# DF1730; RRID: AB_2839084
Anti-PRL	Affinity	Cat# DF6506; RRID: AB_2838468
Anti-MAN1A1	Abcam	Cat# ab102797; RRID: AB_10860970
Anti-SP1	Proteintech	Cat# 21962-1-AP; RRID: AB_10898171
Anti-NPM1	Proteintech	Cat# 10306-1-AP; RRID: AB_2155163
Anti-GAPDH	Bioworld Biotech	Cat# AP0063; RRID: AB_2651132
Critical commercial assays		
Lectin Microarray	Raybiotech	GA-Lectin 70
BCA Protein Assay Kit	Beyotime	P0012S
Prime Script RT reagent kit	Takara	RR037A
SYBR Premix Ex Taq II kit	Takara	DRR041A
RNA pull-down kit	Bersin BIO	Bes5102
Magna RIP kit	Millipore	17-700
Magna ChIP kit	Millipore	17-70085
RNA FISH SA-biotin	Gene Pharma	N/A
PARIS™ kit	Invitrogen	N/A
Experimental models: Cell lines		
HESCs	ATCC	BFN608006424
Chemicals, peptides, and recombinant proteins		
medroxyprogesterone 17-acetate (MPA)	Selleck	S256702
dibutyryl cAMP (dbcAMP)	Selleck	S785811
Golgi-Tracker Red	Beyotime	C1043
GNA	Vector Lab	Cat# L-1240-5; RRID: AB_2336471
Software and algorithms		
ImageJ	National Institutes of Health	https://imagej.nih.gov/ij/
GraphPad Prism 9.0	GraphPad Prism Software	https://www.graphpad.com/
ImageLab	Bio-Rad Laboratories	https://chameleonimagelab.com/
Oligonucleotides		
sense: 5′-GAGACUGACUCAUGAUCCATT-3′ antisense: 5′-UGGAUCAUGAGUCAG UCUCTT-3′	GenePharma	MAN1A1-siRNA
sense: 5′-GGUGUUAUCAAGUGAAUUATT-3′ antisense: 5′-UAAUUCACUUGAUAACA CCTT-3′	GenePharma	lncNEAT1-siRNA
sense:5′-CCAUUAACCUCAGUGCAUUTT-3′ antisense: 5′-AAUGCACUGAGGUUA AUGGT T-3′	GenePharma	SP1-siRNA
sense: 5′-GUGCAAAGGAUGAGUUGCATT-3′ antisense: 5′-UGCAACUCAUCCUUUG CACTT-3′	GenePharma	NPM1-siRNA
5′-AAGTTCGTGCTGCTGCTGGTATTC-3′	Sangon Biotech	MAN1A1-F

(*Continued on next page*)

Continued

REAGENT or RESOURCE	SOURCE	IDENTIFIER
5′-TTGGAGGAGTCTGGCAGGAAGAAG-3′	Sangon Biotech	MAN1A1-R
5′-TGGCTAGCTCAGGGCTTCAG-3′	Sangon Biotech	LncNEAT1-F
5′-TCTCCTTGCCAAGCTTCCTTC-3′	Sangon Biotech	LncNEAT1-R
5′-TATGATGGCTCGAAGGCTCT-3′	Sangon Biotech	IGFBP-1-F
5′-CCATTCTTGTTGCAGTTTGG-3′	Sangon Biotech	IGFBP-1-R
5′-TCTCGCCTTTCTGCTTATTATAAC-3′	Sangon Biotech	PRL-F
5′-CGATTCGGCACTTCAGGAGCTT-3′	Sangon Biotech	PRL-R
5′-TCCTGTTCGACAGTCAGCCGCAT-3′	Sangon Biotech	GAPDH-F
5′-TGCAAATGAGCCCCAGCCTTCTCCA-3′	Sangon Biotech	GAPDH-R
5′-AAAAAAGTCCTAAGCAAGCACAGAA-3′	Sangon Biotech	MAN1A1-F (ChIP)
5′-GAAGCGGCAGGCAGAGTTC-3′	Sangon Biotech	MAN1A1-R (ChIP)
5′-TGAGTTCTGTTGTCTCGATTTCTTT ATACCTTTTGGTTTCCTTGGACATTT TTTTCAATCAGGA-3′	GenePharma	lncNEAT1 probe

RESOURCE AVAILABILITY

Lead contact

Further information and requests for resources and reagents should be directed to and will be fulfilled by the lead contact, Qiu Yan (yanqiu@dmu.edu.cn), Shuai Liu (liushuai@dmu.edu.cn).

Materials availability

This study did not generate new unique reagents.

Data and code availability

- Data reported in this paper will be shared by the lead contact upon request.
- This paper does not report original code.
- Any additional information required to reanalyze the data reported in this paper is available from the lead contact upon request.

EXPERIMENTAL MODEL AND STUDY PARTICIPANT DETAILS

Human specimens

This study protocol of human endometrial tissue samples was approved by the Ethics Committee of the Second Affiliated Hospital of Dalian Medical University (2022-87). The early pregnant group (n = 10) and miscarriage group (n = 10) were from 7 to 10 pregnancy weeks. The early pregnant women with regular menstrual cycle were enrolled, and excluded from other gynecological abnormalities. The miscarriage group included recurrent abortion (n = 5) and first abortion (n = 5). All the miscarriage patients with low serum progesterone level (< 25 ng/ml) were confirmed by ultrasound detection and underwent induced abortion.

Cell lines

Human endometrial stromal cells HESCs (ATCC, USA) were cultured in DMEM/F12 (Gibco, USA) containing 100 μg/ml penicillin, 100 U/ml streptomycin (Sigma, merica) and 10% fetal bovine serum (FBS; Gibco, USA). The cells were maintained at 37°C, 5% CO_2 and 90% humidity in an incubator. To induce decidualization *in vitro*, HESCs were treated with DMEM/F12 containing 2% FBS, 1 μM medroxyprogesterone 17-acetate (MPA; Selleck, USA), and 0.5 mM dibutyryl cAMP (dbcAMP; Selleck, USA) for 72 h.

Animal experiments

Mice (Kunming White Crossing Line, 7∼8 weeks old) were purchased from the Experimental Animal Center of Dalian Medical University (Liaoning, China). All mice were housed under standard environmental conditions of 14 h light and 10 h dark in a controlled room (22∼25°C, 60% humidity). Three females were placed with one male overnight to mate. The day of vaginal plug discovery was recorded as gestation day 0.5 (GD 0.5). On GD 3, the mice were anesthetized and injected with siRNA/cDNA into uterine horn. On GD 7, samples of mouse uterus were collected and soaked in formalin for subsequent experiments. The number of implanted embryos was statistically analyzed. Animal models were approved by the Institute Animal Care and Use Committee of Dalian Medical University (Liaoning, China) (No. AEE21080), and the experiments were carried out in accordance with established institutional guidelines and approved protocols.

METHOD DETAILS

Lectin microarray

Lectin microarray of decidual tissues from early pregnant women (n = 3) and miscarriage patients (n = 3) was performed using Lectin microarray (GA-Lectin-70, Raybiotech, USA). Galanthus nivalis lectin (GNA), were used specifically for recognizes high-mannose N-glycans. Decidual tissues were lysed, labeled with biotin, and quantified with BCA Protein Assay Kit (NCM Biotech, China). After blocking, samples (100 μl) were added to each well and incubated at room temperature for 2 h, followed by incubation with Cy3-equivalent-dye-streptavidin. The fluorescent signal intensity was detected and analysed.

Cell transfection

The MAN1A1-siRNA, lncNEAT1-siRNA, SP1-siRNA, NPM1-siRNA and the plasmids of MAN1A1-cDNA and lncNEAT1-cDNA sequences were designed and synthesized by GenePharma. HESCs were plated onto dishes to 80% confluence and transfected with 2 μg plasmid or siRNA and 3∼8 μg PEI (Mine Bio, China) according to the manufacturer's suggestions. After 18 h, the culture medium was replaced with DMEM/F12 containing 10% FBS. HESCs were transfected with siRNA or cDNA plasmid. After 12 h culturing, the culture medium was changed into decidua induction medium containing MPA and dbcAMP for 72 h. Following experiments, such as western blot and immunofluorescence staining, were performed.

RNA extraction and quantitative PCR (qPCR)

RNA was extracted using Trizol (Takara, Japan) according to the manufacturer's protocol. The concentration of RNA was measured by NanoDrop (Thermo Fisher Scientific, USA). RNA (1 μg) was used for cDNA synthesis with Prime Script RT reagent kit (Takara, Japan), and SYBR Premix Ex Taq II kit (Takara, Japan) was used for qPCR.

Western blot

Protein samples were lysed, and quantified by BCA protein assay kit (Beyotime, China). Equal amounts (50 μg) of samples were electrophoresed in 10% SDS-PAGE gels, and transferred onto nitrocellulose membranes. Membranes were blocked in 5% skimmed milk in TBST for 2 h, and incubated with the following primary antibodies at 4°C overnight: IGFBP-1 (1:500, Affinity, USA), PRL (1:500, Affinity, USA), MAN1A1 (1:1000, Abcam, UK), SP1 (1:1000, Proteintech, China), NPM1 (1:500, Proteintech, China), GAPDH (1:2000, Bioworld Technology, USA) and GNA (1:2000, Vector Laboratories, USA). The secondary antibodies were incubated at room temperature for 1 h as follows: HRP goat anti-rabbit (1:2000) and HRP-conjugated streptavidin (1:2000). An enhanced chemiluminescence detection system (Bio-Rad) was used to visualize immunoreactivity bands.

Immunohistochemistry

After incubation with xylol for deparaffinization and rehydration in descending concentrations of ethanol, the endometrial tissue sections were immersed in EDTA solution for antigen retrieval. The 3% H_2O_2 solution was added to the sections for 15 min to eliminate endogenous peroxidases and then blocked with goat serum for 45 min. The sections were incubated with the following primary antibodies at 4°C overnight: MAN1A1 (1:100) and GNA (1:100), and then incubated with secondary antibody and horseradish-labeled streptomycin successively for 45 min at room temperature. The sections were visualized with diaminobenzidine (DAB) and hematoxylin. Neutral resin was used to seal the sections. Images were captured under an inverted microscope (Olympus, Japan).

Immunofluorescence

The cell coverslips were fixed in 4% paraformaldehyde for 20 min, and then blocked with immunol staining blocking buffer (Beyotime, China) for 1 h. Cell coverslips were incubated with primary antibodies at 4°C overnight as follows: IGFBP-1 (1:100), PRL (1:100), MAN1A1 (1:100) and GNA (1:100). After washing with PBS, cell coverslips were incubated with TRITC-labeled streptavidin (1:100, ZSGB-BIO, China) and FITC-conjugated goat anti-rabbit IgG (1:100, ZSGB-BIO, China) at room temperature for 1 h, and then 4,6-diamidine-2-phenylindole (DAPI, 1:4000; Beyotime, China) was used to stain nuclei for 15 min. Images were visualized under fluorescence microscope (Olympus, Japan).

RNA pull-down

The RNA pull-down assay was performed using RNA pull-down kit (Bersin BIO, China) according to the manufacturer's protocol. The lncNEAT1-biotin probe was designed and synthesized by GenePharma. Whole protein was extracted by RIP buffer from 1×10^7 HESCs. After removing nucleic acids from protein samples, the lncNEAT1-biotin probe and magnetic bead complex were mixed with protein lysates and gently rotated at room temperature for 2 h. Protein elution buffer was added and incubated at 37°C for 2 h. The protein samples were analyzed by LC–MS/MS and western blot.

Immunoprecipitation

Cells were harvested and lysed on ice with immunoprecipitation lysis buffer for 30 min. The extracts were incubated with NPM1 antibody (5 μg) and magnetic bead working buffer, and rotated gently at 4°C overnight. And then the bound proteins were separated by elution buffer and

resuspended in SDS loading buffer. The whole cell lysates and immunoprecipitants were incubated at 70°C for 10 min, followed by western blot.

RNA-binding protein immunoprecipitation (RIP)

RIP assay was performed using Magna RIP RNA-binding protein immunoprecipitation kit (Millipore, America) according to the manufacturer's instructions. Briefly, HESCs were collected and lysed with RIP lysis buffer. After incubation with NPM1 antibody (5 μg) and rabbit IgG (1 μg, as a negative control), the protein A/G magnetic beads were mixed with the cell lysates and gently rotated at 4°C overnight. The NPM1-RNA complexes were purified with RIP wash buffer. The precipitated RNA was detected by PCR.

Chromatin immunoprecipitation (ChIP)

ChIP assay was performed using Magna ChIP kit (Millipore, America) according to the manufacturer's instructions. Briefly, HESCs (1×10^7) were crosslinked with 1% formaldehyde for 10 min at room temperature. The glycine solution was used to stop crosslinking for 10 min. After cells were collected with cell lysis buffer, and then pelleted by centrifugation. Cell pellets were resuspended in nuclear lysis buffer and fragmented to 100∼500 base pairs using an ultrasonic wave vibrator. DNA fragments were incubated overnight with SP1 antibody (5 μg), anti-RNA polymerase (1 μg, as a positive control) and normal mouse IgG (1 μg, as a negative control). The chromatin-antibody complex was incubated with protein A/G magnetic beads for 4 h. The precipitated DNA/protein complexes were eluted from the antibodies/beads by incubation with elution buffer. The purified DNA was used as the template for PCR analysis. The PCR products were detected by agarose gel electrophoresis.

Subcellular fractionation location

The separation of cell nuclear and cytoplasmic fractions was performed by PARIS kit (Invitrogen, America) according to the manufacturer's instructions. Briefly, nucleus and cytoplasm were lysed with cell fractionation buffer or cell disruption buffer, and RNAs were isolated from nucleus and cytoplasm by lysis/binding solution, followed by elution solution. The RNA concentration was measured by NanoDrop and used as the template for PCR.

Fluorescence *in situ* hybridization (FISH)

FISH was used to detect the location and expression of lncNEAT1 in HESCs and endometrial tissues with RNA FISH SA-biotin (Gene Pharma, China) according to the manufacturer's instructions. lncNEAT1-specific probes were obtained from GenePharma. The cell coverslips were fixed with 4% paraformaldehyde, and permeabilized with 0.5% Triton X-100 for 15 min at room temperature. After incubation with blocking buffer, SSC solution was added for 30 min at 37°C. The endometrial tissue sections were incubated with xylol for deparaffinization, and then buffer C containing 1% proteinase K were added for 30 min at 37°C. The sections were incubated with denaturation solution for 8 min at 78°C, followed by rehydration in descending concentrations of ethanol (70%∼100%). The coverslips and endometrial tissue sections were subsequently incubated with lncNEAT1 probe working solution at 37°C overnight. DAPI was used to stain nuclei for 15 min. Images were visualized under a fluorescence microscope.

QUANTIFICATION AND STATISTICAL ANALYSIS

All experiments were repeated at least three times and all quantitative data were expressed as mean ± SEM. Comparisons between two groups were analyzed using Student's t test. One-way ANOVA was used for the comparison of multiple groups, and correlation studies were performed using the Pearson correlation test. Statistical analysis and graph presentation were achieved by using GraphPad Prism 8.0 Software (GraphPad, USA). $p < 0.05$ was considered statistically significant.